MOLECULAR AND CELLULAR BIOLOGY, Dec. 2008, p. 7465–7475 Vol. 28, No. 24
0270-7306/08/$08.00+0 doi:10.1128/MCB.00715-08

Ikaros Represses the Transcriptional Response to Notch Signaling in T-Cell Development▽†

Eva Kleinmann, Anne-Solen Geimer Le Lay, MacLean Sellars, Philippe Kastner,* and Susan Chan*

Institut de Génétique et de Biologie Moléculaire et Cellulaire (IGBMC), Department of Cancer Biology, Illkirch F-67400, France; Inserm U596, Illkirch F-67400, France; CNRS UMR7104, Illkirch F-67400, France; and Université Louis Pasteur, Strasbourg F-67000, France

Received 2 May 2008/Returned for modification 11 June 2008/Accepted 28 September 2008

Notch activity is essential for early T-cell differentiation, but aberrant activity induces T-cell transformation. Thus, Notch target genes must be efficiently silenced in cells where Notch activity is no longer required. How these genes are repressed remains poorly understood. We report here that the Ikaros transcription factor plays a crucial role in repressing the transcriptional response to Notch signaling in T-cell development. Using the Notch target gene Hes-1 as a model, we show that Ikaros and RBP-Jκ, the transcriptional mediator of Notch signaling, compete for binding to two elements in the Hes-1 promoter in immature thymocytes. This antagonistic interaction likely occurs at the CD4$^-$ CD8$^-$ CD3$^-$ double-negative 4 (DN4) stage, where Ikaros levels and binding to the Hes-1 promoter increase sharply and wild-type thymocytes lose their capacity to transcribe Hes-1 upon Notch stimulation. Nonresponsiveness to Notch signaling requires Ikaros, as Ikaros-deficient DN4 and CD4$^+$ CD8$^+$ double-positive (DP) cells remain competent to express Hes-1 after Notch activation. Further, Hes-1 promoter sequences from Ikaros-deficient DP cells show reduced trimethylated H3K27, a modification associated with silent chromatin. These results indicate that Ikaros functions as a transcriptional checkpoint to repress Notch target gene expression in T cells.

The Notch pathway is implicated in the development of many cell types. The activation of this pathway occurs when Notch receptors expressed on the surface of one cell are engaged by ligands expressed on neighboring cells. The intracellular domain of Notch (NIC) then is cleaved by metalloproteases and γ-secretase and is translocated to the nucleus, where it forms a complex with the Notch-specific transcription factor RBP-Jκ/CSL and the cofactor Mastermind to activate the transcription of target genes such as Hes-1 (38).

Notch signaling is essential for the early steps of T-cell development (42). Notch activation is required for the generation and maintenance of DN1 (double-negative CD4$^-$ CD8$^-$ CD3$^-$ ckit$^+$ CD44$^+$ CD25$^-$) cells (33, 44, 47), and Hes-1 expression is induced at this stage (21). Notch signaling also is required in DN2 (ckit$^+$ CD44$^+$ CD25$^+$) and DN3 (ckit$^-$ CD44$^-$ CD25$^+$) cells (46), where target genes such as pTα, Deltex-1, Notch 1, and Notch 3 are highly expressed (16, 23, 41, 51). Furthermore, Notch signaling is required for cell survival and proliferation, T-cell receptor (TCR) β-chain rearrangement, and β selection at the DN3 stage (12, 18, 46). Interestingly, DN4 (CD44$^-$ CD25$^-$) cells appear less dependent on Notch signaling for maturation into the DP (double-positive CD4$^+$ CD8$^+$ TCR$^{lo/med}$) population. Indeed, Notch signaling at the DP stage induces the expansion and leukemic transformation of these cells (1). Thus, Notch target gene expression must be tightly regulated during thymocyte differentiation.

Hes-1 is a basic helix-loop-helix transcription factor that is essential for T-cell development. It is highly expressed in DN thymocytes, is absent in DP cells, and is reexpressed at low levels in mature CD4$^+$ CD8$^-$ and CD4$^-$ CD8$^+$ thymocytes (11, 16, 17). Hes-1 is important for the expansion of DN thymocytes both before and after TCR β-chain rearrangement, and cells lacking Hes-1 are blocked at the DN3 stage of differentiation (27, 49). Studies in other systems indicate that Hes-1 functions simultaneously to promote cell proliferation and inhibit the differentiation of progenitor cells (22, 24, 37). Hes-1 also has been shown to bind the CD4 silencer and repress CD4 transcription in vitro (28), which may explain why its expression is shut off in DP cells.

Although it is generally accepted that the NIC/RBP-Jκ effector complex activates Notch target gene transcription, it is still unclear how the transcription of these genes is turned off. Several scenarios may take place in T cells. First, the thymic environment through which DN4 and DP thymocytes pass may not express sufficient Notch ligands, leading to the loss of Notch signaling and the inactivation of the transcriptional complex (26). Second, RBP-Jκ has been postulated to function as a constitutive transcriptional repressor of Notch target genes in the absence of NIC (4, 8), although recent data suggest that RBP-Jκ binding is transient and dynamically regulated by Notch signaling (32). Third, Notch target genes may be rendered differentially susceptible to Notch activation through epigenetic remodeling during differentiation.

The hematopoietic cell-specific transcription factor Ikaros functions as a key regulator of lymphocyte differentiation and a tumor suppressor in T cells (15, 53). Ikaros colocalizes with heterochromatin and associates with NURD complexes in activated T cells, suggesting a role in gene repression (10, 29, 31). We and others have proposed that Ikaros plays a major role in downregulating Notch target gene expression in transformed T cells (7, 17).

* Corresponding author. Mailing address: IGBMC, BP 10142, 67404 Illkirch Cedex, France. Phone: 33-3-88-65-34-61. Fax: 33-3-88-65-32-01. E-mail: scpk@igbmc.u-strasbg.fr.

† Supplemental material for this article may be found at http://mcb.asm.org/.

▽ Published ahead of print on 13 October 2008.

Ikaros-deficient mice carrying a hypomorphic mutation ($Ik^{L/L}$) in the Ikaros locus develop T-cell lymphomas/leukemias that all exhibit strong activation of Notch target genes (17). Notch activation occurs early in tumorigenesis and may precede transformation. Furthermore, we showed that Ikaros binds to the Notch-responsive TGGGAA element in the Hes-1 promoter and represses Notch-dependent transcription from this promoter in vitro. These experiments suggested that the Ikaros-mediated repression of Notch target gene expression plays a critical role in defining its tumor suppressor function.

In the present study, we asked if Ikaros can modulate Notch signaling in normal T-cell differentiation. Using Hes-1 as a model Notch target gene, we demonstrate that Ikaros and RBP-Jκ compete for binding to common recognition sites in two regions of the Hes-1 promoter in wild-type thymocytes. Ikaros expression peaks in DN4 thymocytes, as these cells become less dependent on Notch signaling for further maturation. High Ikaros levels correlate with an incapacity to transcribe Hes-1 in response to exogenous Notch signaling. Furthermore, Ikaros is required to establish repressive histone modifications in DP cells. These results indicate that Ikaros antagonizes RBP-Jκ to silence Notch target gene expression in T cells.

MATERIALS AND METHODS

Sequence alignment. Input genomic sequences were obtained from http://www.ncbi.nlm.nih.gov/mapview. Mouse and orthologous sequences (human, rat, chimpanzee, and bovine), from −20 kb to +1 kb with respect to the transcriptional start site, were used as the input in a PromAn analysis (http://bips.u-strasbg.fr/PromAn/) (35) and visualized in GeneDoc (http://iubio.bio.indiana.edu/soft/molbio/ibmpc/genedoc-readme.html).

Electrophoretic mobility shift assay (EMSA)-Supershift. Ik1 and RBP-Jκ proteins were produced in transfected COS cells using expression vectors containing Ik1 or RBP-Jκ cDNA. Nuclear extracts were prepared according to Andrews and Faller (3), and 3 to 10 μg was incubated as previously described (17) in the presence or absence of an anti-RBP-Jκ monoclonal antibody (K0043; Institute of Immunology Co. Ltd., Tokyo, Japan) or a homemade anti-Ikaros polyclonal antibody. The following probes were used for the Hes-1 promoter: −100 bp AB, 5′-ACTGTGGGAAAGAAAGTTTGGGAAGTTTCAC; mAB, 5′-ACTGTGCTGCAGAAAGTTTGGGAAGTTTCAC; AmB, 5′-ACTGTGGGAAAGAAAGTTTGCTGCGTTTCAC; −9 kb CD, 5′-CGCTCCTTCCCACGTACCTTACCCTGGGAATTGCTT; mCD, 5′-CGCTCCTTGGCACGTACCTTACCCTGGGAATTGCTT; CmD, 5′-CGCTCCTTCCCACGTACCTTACCCTGCCAATTGCTT; and mCmD, 5′-CGCTCCTTCCCACGTACCTTACCCTGCCAATTGCTT.

Mice. The $Ik^{L/L}$ mouse line was described previously (30). Mice used in this study were backcrossed 10 generations onto the C57BL/6 background.

Antibodies and flow cytometry. To purify DN cells, thymocytes were stained for lineage-positive cells using the following antibodies: anti-CD4 (GK1.5), anti-CD8α (YTS169.4), anti-CD3 (KT3), anti-B220 (RA3-6B2), anti-CD11b (M1/70), anti-Gr1 (RB6-8C5), and anti-NK1.1 (PK136). They were depleted with Dynabeads conjugated to goat anti-rat immunoglobulin G (IgG) (Immunogen). The remaining cells were stained with anti-rat IgG-fluorescein isothiocyanate (FITC) (Jackson Immunoresearch), CD44-Cy5, and CD25-phycoerythrin (CD25-PE) (BD Pharmingen) and were sorted on FITC-negative cells with the indicated phenotypes. To purify DP cells, thymocytes were stained with anti-CD4-PE and anti-CD8-FITC and sorted for $CD4^+$ $CD8^+$ cells. Cell sorting was performed on a FACSVantage SE option DiVa (BD Biosciences). The sort purity was >98%. Labeled cells were analyzed on a FACSCalibur (BD Biosciences). Results were analyzed using FlowJo software (TreeStar).

ChIP. Chromatin immunoprecipitation (ChIP) assays were performed using modified versions of the protocol from Upstate. Antibodies used were specific for acetylated H3 (06-599; Millipore), acetylated H3K9 (07-352; Millipore), dimethylated H3K4 (ab7766; Abcam), trimethylated H3K27 (07-449; Millipore), and NIC1 (2421; Cell Signaling). The Ikaros-specific antibody is a rabbit polyclonal antibody generated in our laboratory. Thymocytes were fixed with 1% formaldehyde for 10 min at 37°C. After being quenched with 125 mM glycine, the fixed cells were washed twice with ice-cold phosphate-buffered saline (PBS). The cell pellet was resuspended in lysis buffer (50 mM Tris pH 8.1, 10 mM EDTA, 1% sodium dodecyl sulfate [SDS]) containing protease inhibitors. After being incubated on ice for 10 min, the nuclei were subjected to sonication to obtain DNA fragments ranging from 300 to 800 bp using a Bioruptor (Diagenode). Soluble chromatin was clarified by centrifugation at 14,000 rpm for 15 min at 4°C. Chromatin fractions (equivalent to 10^6 cells/precipitation) were precleared with 80 μl of protein A- or G-Sepharose for 1 h, followed by incubation overnight with the indicated antibodies. Protein-DNA complexes were bound to protein A- or G-Sepharose beads for 2 h at 4°C. The beads then were washed once each with low-salt wash buffer (20 mM Tris-HCl, pH 8.1, 150 mM NaCl, 2 mM EDTA, 1% Triton X-100, 0.1% SDS), high-salt buffer (500 mM NaCl), LiCl buffer (10 mM Tris-HCl, pH 8.1, 1 mM EDTA, 1% deoxycholate, 1% NP-40, 0.25 M LiCl), and twice with Tris-EDTA (TE). Protein-DNA complexes were eluted in 500 μl of 1% SDS, 0.1 M $NaHCO_3$, and cross-linking was reversed by adding NaCl to 0.2 M for 4 to 6 h at 65°C. Protein components were removed by proteinase K digestion (2.5 μg) for 1 h at 45°C before phenol-chloroform extraction and precipitation. DNA was resuspended in 400 μl H_2O and subjected to real-time PCR analysis.

For small cell numbers, a modified version of the Agilent protocol was used. Thymocytes (0.5×10^6 to 1×10^6 cells) and *Drosophila melanogaster* Schneider cells (4×10^6 to 4.5×10^6) were cross-linked with formaldehyde for 20 min at 25°C. After being quenched, the cells were lysed in three successive buffers (buffer 1, 50 mM HEPES, 140 mM NaCl, 1 mM EDTA, 10% glycerol, 0.5% NP-40, 0.25% Triton X-100 for 10 min at 4°C; buffer 2, 10 mM Tris-HCl, 200 mM NaCl, 1 mM EDTA, 0.5 mM EGTA for 10 min at room temperature; buffer 3, 10 mM Tris-HCl, 100 mM NaCl, 1 mM EDTA, 0.5 mM EGTA, 0.1% deoxycholate, 0.5% *N*-lauroylsarcosine) before sonication. Soluble chromatin was supplemented with 1% Triton X-100 and clarified by centrifugation. Chromatin fractions were precleared with protein A Sepharose and incubated with the antibody for 4 h at 4°C, and protein-DNA complexes were bound to protein A-Sepharose overnight at 4°C. Protein-DNA complexes were eluted with 450 μl of 1% SDS, 0.1 M $NaHCO_3$ for the Sepharose beads and 210 μl of 50 mM Tris-HCl, 10 mM EDTA, 1% SDS for the Dynabeads. ChIP DNA was resuspended in 100 μl TE, and input DNA was resuspended in 200 μl.

Reactions were performed in triplicate with 5 μl of the eluate (or in duplicate with 2 μl using the Agilent protocol) using SYBR green JumpStart TaqReadyMix (Sigma) and the LightCycler 480 real-time PCR system (Roche). The input template was diluted 1/10. PCRs were analyzed with the LightCycler 480 basic software, and the concentration of amplified DNA was calculated relative to a standard curve obtained with serial dilutions of a control genomic DNA (T-cell DNA). The following calculations were used: percentage input ($\%I$) = $100 \times$ [(antibody bound) − (IgG bound)]/($I \times 10$). The histone modification index for amplicon X was $\%I/\%I_{ref}$, where $\%I_{ref}$ corresponds to the value measured for the amplicon located at bp −100 in the wild-type (WT) sample. Primers used are the following: Hes-1 −100 bp, 5′-CCTCCCATTGGCTGAAAGT, 5′-AGCTCCAGATCCTGTGTGATCC; Hes-1 −1000 bp, 5′-ACGCACGCACACACACACATCCTCT, 5′-CCGAGCTGCAGTTTGACAT; Hes-1 −2700 bp, 5′-CAAGGGTCTTGTGTGTGGTG, 5′-TATGGCTGAGGTGTTGGAAA; Hes-1 −4000 bp, 5′-ACGGGTGGTGGGTTACACT, 5′-TACTCCCAAAGCAGGAGGAA; Hes-1 −6500 bp, 5′-ACACACACACACACCCTGCT, 5′-GTCAAGACCCACCCGAGTTA; Hes-1 −8500 bp, 5′-CTCCCGCATACTAGGTGCTC, 5′-GACTGGTCTGTTGCCTTGGT; Hes-1 −9100 bp, 5′-TTACCCTGGGAATTGCTTTG, 5′-CAGCACCCTCCTGGATACTC; CD8α −1 kb, 5′-TTTCAATTCCTCCCACTTGC, 5′-TTTAGCCAGCTGCAGACAGA.

Real-time reverse transcription-PCR (RT-PCR). Total RNA was isolated from 1×10^5 to 2×10^5 sorted cells using the RNeasy kit (Qiagen) and was resuspended in 12 μl H_2O. RNAs were reverse transcribed with SuperScript II reverse transcriptase (Invitrogen). cDNA corresponding to 10^4 cells was used for Hes-1 amplification. Real-time PCR was performed in duplicate with the Quantitect SYBR green PCR kit (40 cycles of 95°C for 30 s, 58°C for 30 s, and 72°C for 30 s; Qiagen). Hypoxanthine phosphoribosyltransferase (HPRT) cDNAs were amplified with similar conditions, using 50-fold-diluted cDNAs. Hes-1 Quantitect primers were purchased from Qiagen. The HPRT primers were 5′-GTTGGATACAGGCCAGACTTTGTTG (forward) and 5′-GATTCAACTTGCGCTCATCTTAGGC (reverse).

Western blotting. Cell pellets were resuspended in 1× loading buffer (0.33 M Tris, pH 6.8, 10% glycerol, 1.5% SDS, 1.5% 2-mercaptoethanol), and lysates were run on 6 to 10% SDS-polyacrylamide gels. After transfer, the polyvinyl difluoride membranes (Millipore) were blotted overnight with antibodies specific for cleaved Notch 1 (2421; Cell Signaling), RBP-Jκ (T6719; Institute of Immunology), Ikaros, or β-actin (A5441; Sigma). All secondary antibodies were horseradish conjugated (Jackson Immunoresearch). The blots were revealed with

Immobilon Western chemiluminescent horseradish peroxidase substrate (Millipore).

Immunofluorescence staining. Immunofluorescence staining was performed as previously described (30). Samples were mounted in a 1% DAPI (4′,6′-diamidino-2-phenylindole)-Vectashield solution (Vector Labs) and visualized at ×63 with a Leica fluorescence microscope.

Single-cell RT-PCR. The single-cell RT-PCR protocol was adapted from Correia-Neves et al. (14). Cells were sorted into 96-well plates containing 10 μl of RT buffer/well (50 mM Tris-HCl, pH 8.3, 75 mM KCl, 3 mM $MgCl_2$, 10 mM dithiothreitol, 500 μM deoxynucleoside triphosphates, 1% Triton X-100, 10 U rRNasin RNase inhibitor [Promega], 0.5 μM reverse primer, and 40 U SuperScript II reverse transcriptase [Invitrogen]). Immediately after being sorted, plates were spun for 3 min at 2,300 rpm and incubated for 90 min at 37°C in a humidified incubator. For the first PCR, a mix of 40 μl of PCR buffer (1× GoTaq Polymerase Buffer), 200 μM deoxynucleoside triphosphates, 2 μM forward and reverse primers, and 2 U GoTaq polymerase (Promega) was added to each well. Plates were heated for 5 min at 94°C, subjected to 40 PCR cycles (30 s at 94°C, 30 s at 60°C, and 30 s at 72°C), and heated for 10 min at 72°C. For the second PCR, 3 μl of the first-round product was used to amplify Hes-1 or β-actin in separate reactions with the cognate nested primers (50-μl reaction mixture). Products were visualized on 2% agarose gels.

Primers used were the following (5′ to 3′): Hes-1 forward, ACACCGGACA AACCAAAGAC; Hes-1 reverse, TGATCTGGGTCATGCAGTTG; Hes-1 nested forward, GAGCACAGAAAGTCATCAAAGC; Hes-1 nested reverse, CCTCACACGTGGACAGGAA; β-actin forward, CCCTGAAGTACCCCATT GAA; β-actin reverse, GGGCACAGTGTGGGTGAC; β-actin nested forward, TGTTACCAACTGGGACGACA; and β-actin nested reverse, GGGGTGTTG AAGGTCTCAAA.

RESULTS

Ikaros and RBP-Jκ bind to two distinct regions of the Hes-1 promoter. Sequence alignment analyses showed four potential common binding sites for Ikaros and RBP-Jκ in the Hes-1 promoter that were perfectly conserved across murine, human, rat, chimpanzee, and bovine genomes (Fig. 1A). Sites A and B, previously described by Jarriault et al. (25), were separated by 8 bp and were located within 100 bp 5′ of the transcriptional start site. Sites C and D were separated by 12 bp and were located near −9 kb. All sites contained the TGGGAA sequence in forward or reverse (site C) orientation.

To determine if these sites interacted directly with Ikaros and RBP-Jκ, we performed EMSA using probes containing the physiological sequences (Fig. 1B) and protein extracts from transfected COS cells expressing RBP-Jκ or Ik1 (the longest and most abundant Ikaros isoform in T cells). Both RBP-Jκ and Ikaros bound a sequence containing sites A and B with distinct migration profiles (Fig. 1C, lanes 1 to 3), in agreement with our previous findings (17). Both proteins also strongly bound a probe containing sites C and D (lanes 4 to 6). Protein binding was specific, as RBP-Jκ and Ikaros binding to either the proximal or distal sequence could be supershifted using anti-RBP-Jκ and anti-Ikaros antibodies (see Fig. S1 in the supplemental material). RBP-Jκ always bound as a single complex, presumably as a monomer (39), while Ikaros binding produced several complexes likely to be monomeric or multimeric in nature. Furthermore, endogenous RBP-Jκ was not part of the Ikaros complexes, as anti-RBP-Jκ antibodies could not supershift these bands (see Fig. S1 in the supplemental material).

To determine the binding requirement for individual sites, we tested the capacity of RBP-Jκ and Ikaros to bind probes singly or doubly mutated at the indicated sites. RBP-Jκ bound less strongly to the proximal sequences containing a mutated site B and lost all binding to sequences containing a mutated site A (Fig. 1D, lanes 4 to 6), suggesting that RBP-Jκ requires mostly site A for binding. In contrast, Ikaros bound sequences containing a mutated site A (lane 8) but not sequences containing a mutated site B (lane 9), indicating that Ikaros requires predominantly site B for binding. These results are in agreement with our previous findings (17). At −9 kb, RBP-Jκ binding was unchanged when site D was mutated, was reduced when site C was mutated, and was abolished when both sites were mutated (Fig. 1E, lanes 1 to 4 and 9 to 12). Thus, each individual site mediated RBP-Jκ binding in this element. In contrast, both sites were required for efficient Ikaros binding as a high-molecular-weight complex, as the loss of either site reduced binding efficiency (Fig. 1E, lanes 5 to 8).

Our observation that RBP-Jκ and Ikaros share binding sites on the proximal and distal elements raised the possibility that they compete for binding to the Hes-1 promoter. To test this, we performed competitive EMSA, in which increasing quantities of Ikaros were added to fixed amounts of RBP-Jκ in the reaction mixture together with limiting amounts of probe. As shown in Fig. 1F, Ikaros effectively competed with RBP-Jκ to bind both the −100 bp and the −9 kb sequences as RBP-Jκ complexes disappeared, while Ikaros-like complexes appeared when Ikaros was increased. Importantly, no new complexes involving both RBP-Jκ and Ikaros were seen. These results indicate that both RBP-Jκ and Ikaros can bind the proximal and distal elements separately but not together, presumably due to direct competition or steric hindrance.

To investigate if WT thymocytes contained Ikaros proteins capable of binding the Hes-1 promoter, we prepared nuclear extracts from bulk WT or Ikaros-deficient $Ik^{L/L}$ thymocytes and subjected them to EMSA using probes corresponding to the proximal site (Fig. 2A). WT extracts showed a complex binding profile that was consistent with the presence of both Ikaros (black arrows) and RBP-Jκ (white arrows) complexes (compare lane 1 to lanes 13 and 15). The specificity of Ikaros-like complexes was confirmed by other criteria: they were absent when site B was mutated, strongly reduced when $Ik^{L/L}$ extracts were used, and supershifted with an anti-Ikaros antibody. In addition, WT and $Ik^{L/L}$ extracts yielded a prominent band that migrated similarly to RBP-Jκ, which still was seen using a probe with mutated site B; this complex was entirely supershifted with an anti-RBP-Jκ antibody (Fig. 2A; also see Fig. S2 in the supplemental material). These experiments show that Ikaros and RBP-Jκ are the major endogenous factors in WT thymocytes that can bind strongly to the proximal Hes-1 promoter in vitro.

To determine if Ikaros bound the Hes-1 promoter in vivo, we performed high-resolution ChIP experiments on purified subpopulations of WT thymocytes. Protein-DNA complexes from immature DN (Lin^- $CD4^-$ $CD8^-$ $CD3^-$ $B220^-$ $Gr1^-$ $CD11b^-$ $NK1.1^-$) and more mature DP ($CD4^+$ $CD8^+$) thymocytes were immunoprecipitated using antibodies specific for Ikaros or intracellular cleaved Notch 1 (NIC1), a cofactor of the RBP-Jκ activation complex (note that ChIPs using anti-RBP-Jκ antibodies were inconclusive). RT-PCR was performed to amplify distinct sequences spanning the Hes-1 promoter from −10 kb to the transcriptional start site (Fig. 2B). In DN cells, anti-NIC1 antibodies efficiently precipitated DNA sequences corresponding to the proximal and −9 kb regions of the Hes-1 promoter but not sequences in between, demonstrat-

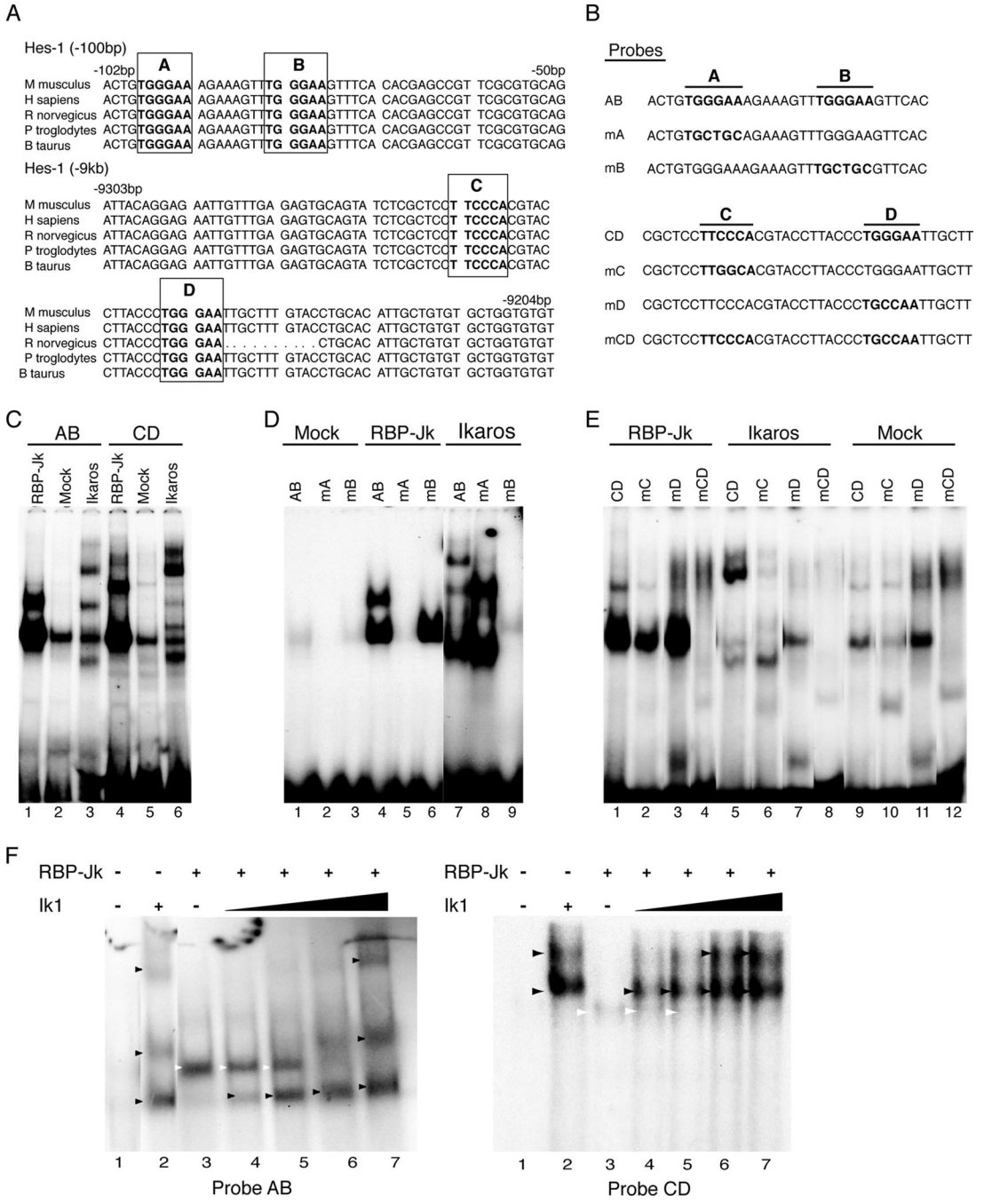

FIG. 1. Ikaros and RBP-Jκ bind and compete for common sites in the Hes-1 promoter. (A) Alignment of mammalian Hes-1 promoters (murine, human, rat, chimpanzee, and bovine [*Mus musculus*, *Homo sapiens*, *Rattus norvegicus*, *Pan troglodytes*, and *Bos taurus*, respectively]). TGGGAA and the reverse-orientation TTCCCA sequences at the indicated regions are marked in boldface and are boxed. (B) EMSA probe sequence. (C to E) Binding of Ikaros and RBP-Jκ to indicated Hes-1 sequences. (F) Competition between Ikaros and RBP-Jκ at the proximal (left) and distal (right) promoters by EMSA. Arrows indicate the different protein complexes (black arrows for Ikaros, white arrows for RBP-Jκ). All assays were performed using 3 μg of nuclear extracts from COS cells transfected with an empty (mock) or Ik1- or RBP-Jκ-containing expression vector. (F) RBP-Jκ was fixed at 3 μg, while Ikaros proteins were serially increased from 0.12 to 1 μg. All results are representative of at least three similar experiments.

ing that both elements are specifically bound by the RBP-Jκ/NIC1 complex in immature thymocytes (Fig. 2C). Similarly, anti-Ikaros antibodies precipitated DNA sequences corresponding to these regions but not the intervening sequences (Fig. 2D). In contrast, neither anti-NIC1 nor anti-Ikaros antibody precipitated convincing amounts of DNA above background levels from DP cells (data not shown) (Fig. 3D). These results demonstrate that both the RBP-Jκ activation complex and Ikaros bind common recognition sequences in two distinct regions of the Hes-1 promoter. This binding is specific and

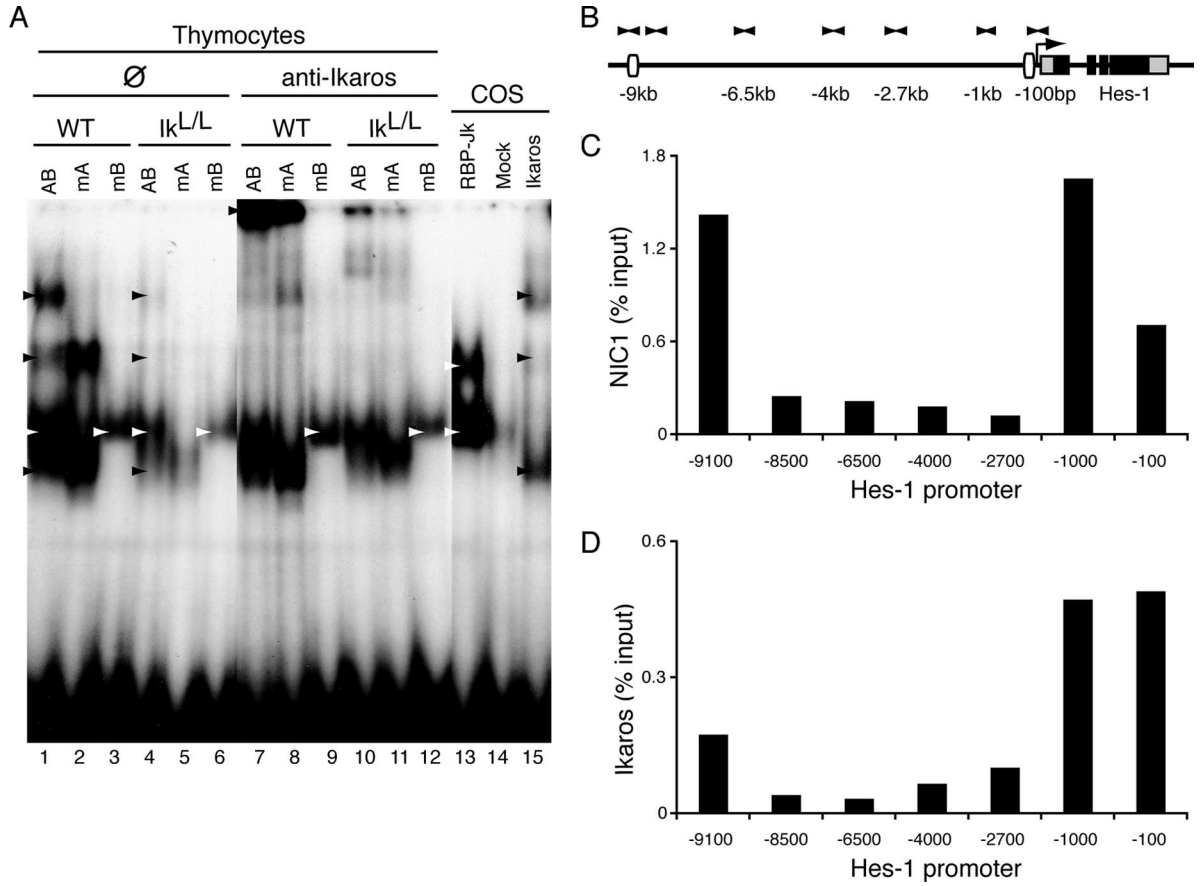

FIG. 2. Ikaros and RBP-Jκ bind to the Hes-1 promoter in WT thymocytes. (A) Binding of Ikaros and RBP-Jκ proteins, extracted from WT thymocytes, to the proximal Hes-1 promoter by EMSA. Black arrows, Ikaros complexes; white arrows, RBP-Jκ complexes. Results are representative of three similar experiments. (B) Diagram of the Hes-1 locus and location of the real-time PCR primers used for analysis of ChIP assays. An arrowhead pointing to the right signifies 5′ to 3′ primers; an arrowhead pointing to the left signifies 3′ to 5′ primers. (C and D) ChIP experiments on protein-DNA complexes precipitated by antibodies specific for cleaved Notch 1 (C) or Ikaros (D) from WT DN thymocytes. Data shown are from one representative experiment out of four that gave similar results.

competitive, and it appears to be physiologically regulated during thymocyte differentiation.

Ikaros is dynamically upregulated during the DN3-DN4-DP transition in WT thymocytes. Since Notch signaling is required for DN1 to DN3 differentiation but appears to be dispensable at the DN4 stage, we asked if there were differences in the amounts of Ikaros and RBP-Jκ expressed in thymocytes during this transition period. WT DN3 ($CD44^-$ $CD25^+$ Lin^-), DN4 ($CD44^-$ $CD25^-$ Lin^-), and DP ($CD4^+CD8^+$) cells were sorted and analyzed for Ikaros and RBP-Jκ by Western blotting (Fig. 3A, B). While Ikaros proteins were detected in all populations, their levels were significantly higher in DN4 than in DN3 and DP cells. Interestingly, bands corresponding to larger-size proteins were detected by the Ikaros antibody in DN4 cells, suggesting that Ikaros is posttranslationally modified in these cells. Furthermore, almost all DN4 cells showed high levels of Ikaros proteins, while few DN3 and DP cells showed similarly high-level staining when analyzed at the single-cell level by immunofluorescence (Fig. 3C). In contrast, RBP-Jκ protein levels remained similar across these populations in both WT (Fig. 3B) and Ikaros-deficient $Ik^{L/L}$ cells (see Fig. S3 in the supplemental material). These results demonstrate that Ikaros specifically accumulates in DN4 thymocytes, thereby increasing the relative ratio between Ikaros and RBP-Jκ at this stage of differentiation.

To investigate if increased Ikaros levels correlated with enhanced binding to the Hes-1 promoter in vivo, we performed ChIP experiments on purified populations of WT DN3, DN4, and DP cells. Ikaros binding was at background levels in DN3 cells, strikingly upregulated in DN4 cells at the −9 kb and −100 bp regions, and undetectable in DP cells (Fig. 3D). The reduction in DP cells was not due to technical problems, as we consistently recovered sequences in the promoter of CD8α (see Fig. S4 in the supplemental material), a bona fide Ikaros target gene in these cells (20). These findings strongly suggest that Ikaros interacts directly with the Hes-1 promoter in DN4 cells to control Hes-1 transcription.

Nonresponsiveness to exogenous Notch signals in WT, but not $Ik^{L/L}$, DN4 and DP thymocytes. To determine if fluctuations in Ikaros levels and promoter binding affect Hes-1 mRNA expression in thymocyte populations, DN3, DN4, and DP cells were freshly isolated from WT and $Ik^{L/L}$ thymuses and subjected to real-time RT-PCR analyses for Hes-1 expression (Fig. 4A, B; note that the DN4 population is always increased

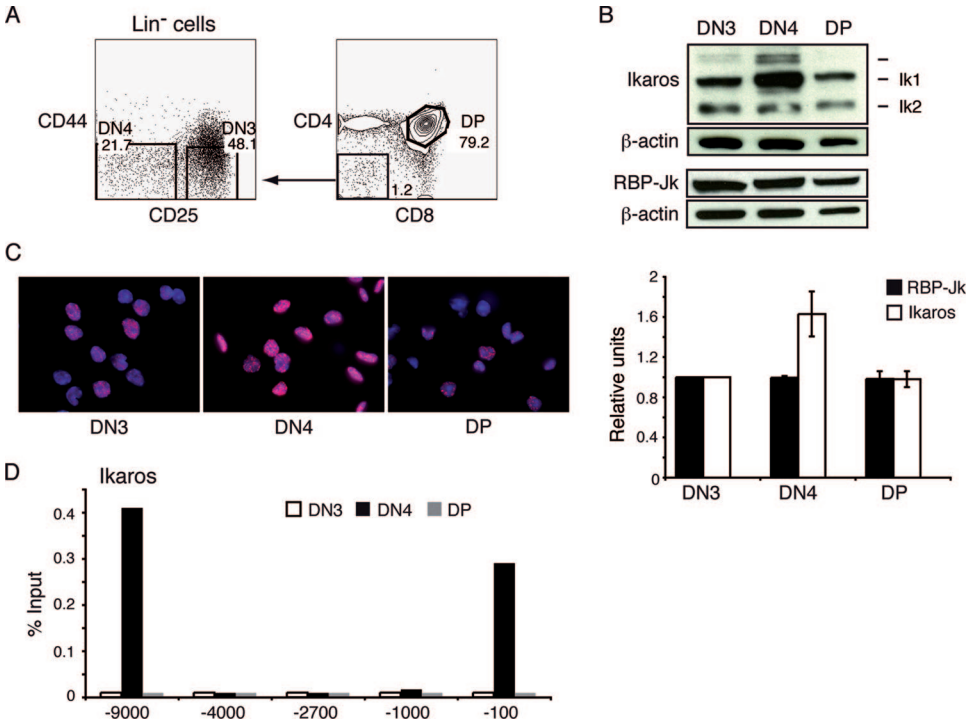

FIG. 3. Ikaros is highly expressed in WT DN4 thymocytes. (A) Sorting gates for DN3, DN4, and DP cells. Thymocytes were pooled from 8 to 10 WT mice at 5 to 7 weeks of age. DN3 cells are defined as Lin^- $CD44^-$ $CD25^+$, DN4 cells as Lin^- $CD44^-$ $CD25^-$, and DP cells as $CD4^+$ $CD8^+$. Lineage (Lin) markers are CD4, CD8, CD3, B220, CD11b, Gr1, and NK1.1. (B) Ikaros and RBP-Jκ protein levels in the indicated populations, as detected by Western blotting. β-Actin was used as a loading control. The bar graph depicts the quantities of Ikaros and RBP-Jκ proteins relative to those of the DN3 population, which were defined as 1.0. Protein levels were normalized to β-actin using Tina 2.0 software. Means and standard deviations were obtained from three independent experiments for Ikaros and two experiments for RBP-Jκ. (C) Ikaros protein levels at the single-cell level, as detected by the immunofluorescence of the indicated populations ($n = 3$). (D) ChIP experiments on protein-DNA complexes precipitated by antibodies specific for Ikaros from WT DN3, DN4, or DP thymocytes. Real-time PCR was performed using the Hes-1 promoter amplicons depicted in Fig. 2B ($n = 3$).

in $Ik^{L/L}$ mutants, similarly to previous reports on Ikaros null mice [52]). In addition, we measured the levels of Notch signaling received by each population by Western blotting using an antibody specific for cleaved Notch 1 (Fig. 4C).

In WT cells, Hes-1 mRNA levels were highest in DN3 cells, significantly decreased in DN4 cells (26-fold), and almost undetectable in DP cells. In direct correlation, NIC1 protein levels also were highest in DN3 cells, significantly decreased in DN4 cells, and undetectable in DP cells. These results are consistent with previous findings that Hes-1 is a Notch target gene and requires active Notch signaling for transcription (16). In $Ik^{L/L}$ DN3 cells, Hes-1 expression was similar to that observed in WT DN3 cells. However, Hes-1 expression in the $Ik^{L/L}$ DN4 and DP populations, though lower than that detected in $Ik^{L/L}$ DN3 cells, remained significantly higher than the levels seen in the corresponding WT populations (4- and 20-fold, respectively). Importantly, cleaved Notch 1 proteins were detected at similar levels in $Ik^{L/L}$ and WT DN4 cells and were undetectable in the DP population in both types of mice. These data suggest that reduced Ikaros function influences the efficient downregulation of Hes-1 during the DN3 to DP transition, even as Notch signaling is unchanged.

Higher Hes-1 expression in the $Ik^{L/L}$ cells could be due to the very high expression of this gene in a few cells (i.e., early transformed cells) or higher numbers of cells expressing Hes-1 upon Notch signaling. To address this issue, we directly assessed the intrinsic responsiveness of differentiating thymocytes to Notch signaling at the single-cell level. WT and $Ik^{L/L}$ thymocytes were artificially provided Notch signals in a coculture system with OP9-DL1 cells, which express the Notch ligand Delta-like1 (45). Thymocytes cultured for 12 h on OP9-DL1 or OP9-GFP cells were purified into DN3, DN4, or DP populations and subjected to single-cell RT-PCR for the simultaneous detection of Hes-1 and β-actin (Fig. 5A).

After 12 h on OP9-GFP cells, both WT and $Ik^{L/L}$ thymocytes behaved similarly: Hes-1-positive cells were few in the DN3 and DN4 populations (<10%) and extremely rare in DP cells. After 12 h on OP9-DL1 cells, however, $Ik^{L/L}$ thymocytes showed a strikingly different pattern of Hes-1 expression compared to that of WT cells. In WT samples, large numbers of cells expressed Hes-1 in the DN3 population; very few cells expressed this gene in the DN4 population, and positive cells were practically absent in the DP population (DN3, 61%; DN4, 4.1%; DP, 0.5% [mean percentages]), indicating that Notch target gene expression cannot be induced by Notch signals in the more mature DN4 and DP thymocyte populations. In contrast, significant numbers of $Ik^{L/L}$ cells expressed Hes-1 in all populations tested, and this was particularly evident in the DN4 and DP populations (DN3, 81%; DN4, 19.3%; DP, 15.3% [mean percentages]). These results demonstrate that (i) both

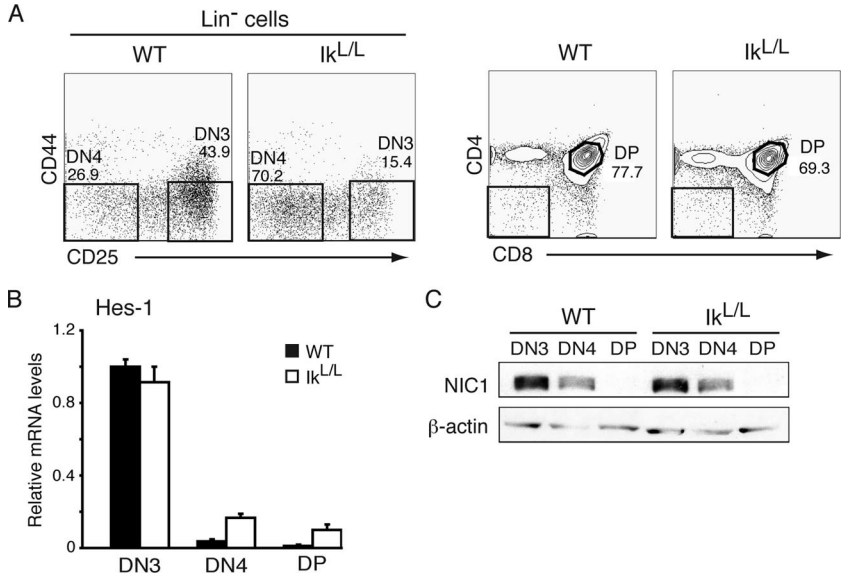

FIG. 4. Hes-1 expression in WT and $Ik^{L/L}$ thymocyte populations. (A) Sorting gates for DN3, DN4, and DP cells. Thymocyte subpopulations were sorted from WT or $Ik^{L/L}$ mice at 3 weeks of age. See the legend to Fig. 3A for details. (B) Hes-1 mRNA expression as measured by real-time RT-PCR on the indicated populations. Results were normalized to HPRT levels, and expression is displayed relative to that of the WT DN3 population, where Hes-1 expression was arbitrarily defined as 1.0. Means and standard deviations were obtained from two independent experiments. (C) Cleaved Notch 1 (NIC1) protein levels as measured by Western blotting of the indicated populations. β-Actin was used as a loading control. Results are representative of three similar experiments.

WT and $Ik^{L/L}$ DN3 cells can be similarly induced to transcribe Hes-1 upon Notch signaling, and (ii) significant numbers of Ikaros-deficient thymocytes retain this responsiveness throughout the DN-DP transition, while WT thymocytes do not.

To test if Notch signaling is modulated by various levels of Ikaros, we analyzed Hes-1 induction in WT, $Ik^{+/L}$, and $Ik^{L/L}$ DN4 cells at the single-cell level using the same experimental setup as that described above (Fig. 5B). Strikingly, Hes-1-positive cells were detected at similarly high frequencies in both the $Ik^{+/L}$ and $Ik^{L/L}$ DN4 populations (18.3 and 18.7%

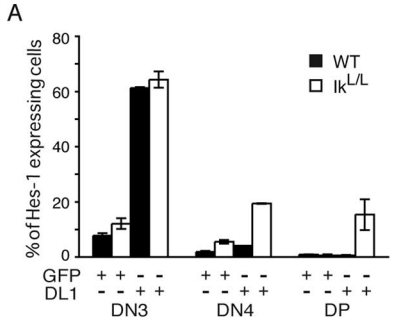

		GFP		DL1	
		Exp 1	Exp 2	Exp 1	Exp 2
WT	DN3	12 / 187	16 / 177	111 / 183	115 / 186
	DN4	4 / 166	2 / 149	7 / 170	6 / 147
	DP	3 / 442	2 / 194	3 / 350	1 / 427
$Ik^{L/L}$	DN3	20 / 135	17 / 181	126 / 184	124 / 173
	DN4	11 / 169	7 / 154	34 / 177	31 / 159
	DP	3 / 269	0 / 336	79 / 340	25 / 334

	GFP		DL1	
	Exp 3	Exp 4	Exp 3	Exp 4
WT	2 / 152	2 / 111	12 / 176	11 / 140
+/L	2 / 190	2 / 180	36 / 189	22 / 124
L/L	3 / 150	5 / 138	34 / 152	12 / 77

FIG. 5. Induction of Hes-1 in single WT, $Ik^{+/L}$, and $Ik^{L/L}$ thymocytes upon exogenous Notch signaling. (A) Single-cell multiplex RT-PCR for Hes-1 and β-actin was performed on WT and $Ik^{L/L}$ thymocytes cultured for 12 h on OP9-GFP or OP9-DL1 stromal cells. Cells from the indicated populations then were sorted as described in the legend to Fig. 3A. Means and standard deviations were obtained from the right panel, which shows the numbers of Hes-1-expressing cells as a ratio with β-actin-expressing cells for the indicated populations and conditions. Two experiments are shown. (B) Using the same experimental setup, WT, heterozygous $Ik^{+/L}$, and homozygous $Ik^{L/L}$ DN4 cells were analyzed for Hes-1 and β-actin expression. Means and standard deviations were obtained from the right panel, which shows the numbers of Hes-1-expressing cells as a ratio with β-actin-expressing cells. Two experiments are shown.

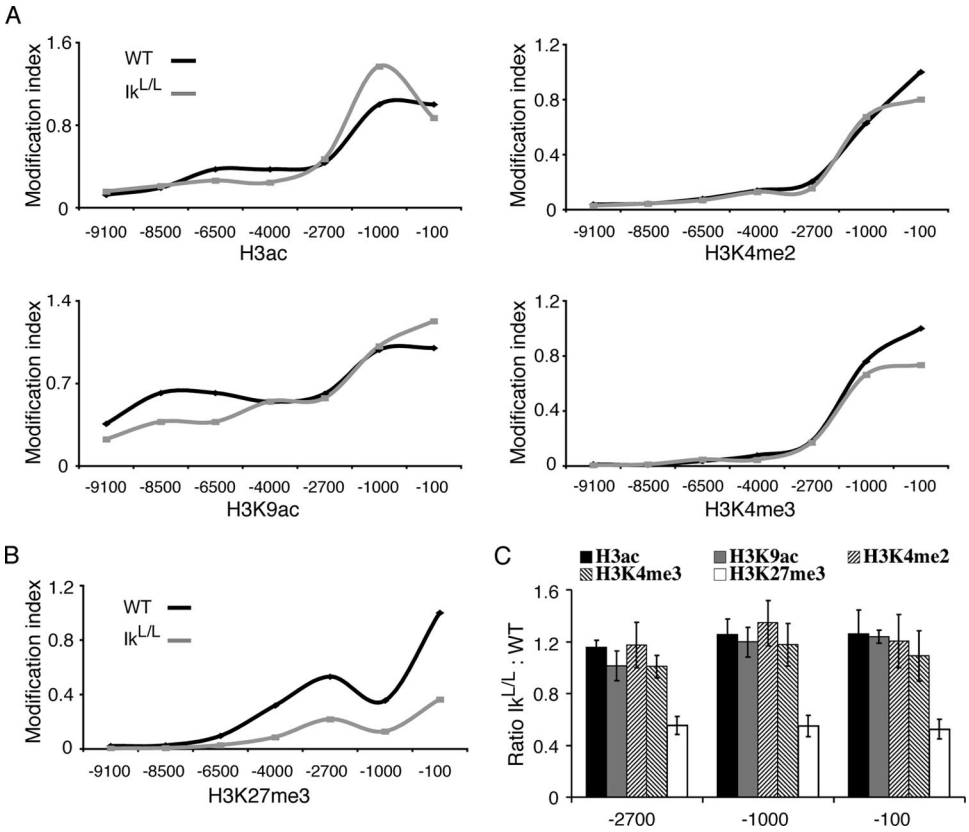

FIG. 6. Hes-1 promoter lacks repressive modifications on histone H3K27 in $Ik^{L/L}$ DP cells. (A and B) Profile of activation (A) and repression (B) marks along the Hes-1 promoter in a representative experiment. WT and $Ik^{L/L}$ DP cells were sorted and subjected to ChIP analysis using antibodies specific for pan-acetylated histone H3 (H3ac), acetylated H3K9 (H3K9ac), dimethylated H3K4 (H3K4me2), trimethylated H3K4 (H3K4me3), and trimethylated H3K27 (H3K27me3), as indicated. Real-time PCR was performed using the Hes-1 promoter amplicons depicted in the legend to Fig. 2B. (C) Ratio of $Ik^{L/L}$ to WT values obtained from the ChIP assays for the indicated antibodies and Hes-1 promoter regions from three independent experiments.

[mean percentages], respectively), while significantly fewer Hes-1^+ cells were detected in the WT samples (7.3%). Furthermore, Hes-1 derepression on the heterozygote background occurs in bona fide DN4 cells and not aberrant DN3-like cells that have bypassed the pre-TCR checkpoint (see Fig. S5 in the supplemental material). These results clearly demonstrate that nonresponsiveness to Notch signals at the DN4 stage is dependent on high levels of Ikaros, although a dose-dependent response in terms of the level of Hes-1 induction between heterozygote and homozygote cells could not be evaluated in these assays.

Ikaros deficiency is associated with reduction of the H3K27 repression mark on the Hes-1 promoter. To investigate why $Ik^{L/L}$ thymocytes, but not WT cells, can still respond to Notch signaling at the DP stage, we analyzed active and repressive histone marks on the Hes-1 promoter in WT and $Ik^{L/L}$ DP thymocytes by ChIP. Activation marks were measured using antibodies specific for pan-acetylated H3, acetylated H3K9, dimethylated H3K4, and trimethylated H3K4. Repression marks were measured using antibodies specific for dimethylated H3K9 (not shown) and trimethylated H3K27. Immunoprecipitated DNA from distinct sequences spanning the Hes-1 promoter from −10 kb to the transcriptional start site was analyzed by real-time PCR (Fig. 2B and 6). There were no clear changes in activation marks between WT and $Ik^{L/L}$ cells (Fig. 6A, C). In contrast, antibodies to trimethylated H3K27 precipitated significantly less DNA from mutant DP cells than did WT DP cells (~50% less; $P = 0.003$ by Student's t test) (Fig. 6B, C). These results suggest that Ikaros is required to establish the trimethyl H3K27 repressive epigenetic mark on the Hes-1 promoter in DP thymocytes.

DISCUSSION

In this report, we used the Hes-1 gene as a model to show that Ikaros is a critical repressor of Notch activity in developing T cells. We demonstrate that the Hes-1 gene does not respond to Notch signals in WT DN4 thymocytes, even though these cells have been shown to express high levels of Notch receptors (6). This unresponsiveness is dependent on optimum levels of Ikaros, as DN4 cells with reduced Ikaros levels express Hes-1 when stimulated with a Notch ligand. Furthermore, Ikaros-dependent silencing is associated with increased levels of trimethylated H3K27, an epigenetic modification linked to Polycomb-mediated repression. Importantly, Ikaros-dependent silencing correlates with a sharp increase in Ikaros protein levels at the DN4 stage and binding to the Hes-1 promoter. Thus, Ikaros appears to play a critical role in DN4 cells by

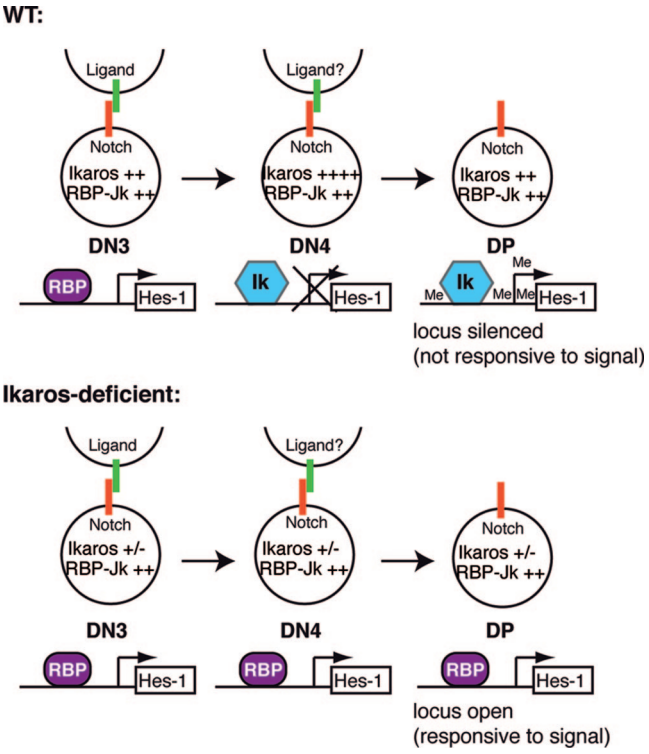

FIG. 7. Modulation of Notch signaling in early T-cell differentiation. Notch activation appears to be regulated via two checkpoints. The first checkpoint occurs at the level of Notch receptor signaling, where thymocytes are subject to interactions between various Notch ligands and receptors. A second checkpoint occurs at the transcriptional level, where Ikaros competes with RBP-Jκ to modulate the transcription of Notch target genes such as Hes-1. In DN4 cells, increased Ikaros levels outcompete RBP-Jκ for binding; histone modification complexes are recruited and chromatin remodeling may occur, leading to the silencing of the Hes-1 locus. In DP cells, this gene is no longer responsive to Notch signaling because it is in a closed chromatin state. In $Ik^{L/L}$ DN4 cells, RBP-Jκ is not displaced from the Hes-1 locus due to insufficient Ikaros proteins. No histone modifications occur. The gene remains in an open state and is sensitive to further Notch signaling. Me, trimethylated H3K27.

limiting their response to Notch signals through epigenetic silencing.

The mechanism by which Ikaros exerts repression probably involves competition with RBP-Jκ for common binding sites in the Hes-1 promoter. We have shown that (i) both Ikaros and RBP-Jκ bind to two regulatory elements in the Hes-1 promoter in vitro, and binding is mutually exclusive; (ii) Ikaros and RBP-Jκ are the only major factors that bind the proximal Hes-1 regulatory element in thymocyte extracts; (iii) Ikaros preferentially binds Hes-1 in the DN4 population, which correlates with an increase in Ikaros levels in these cells; (iv) Ikaros competes with RBP-Jκ to repress the transcription of the Hes-1 promoter in transfection experiments (17). Together, these data provide strong support for Ikaros/RBP-Jκ competition in vivo, although other more complex scenarios cannot be excluded at the present time.

Thus, Notch activation in early T-cell differentiation appears to be regulated via at least two checkpoints (Fig. 7). The first checkpoint occurs at the level of Notch receptor signaling, where thymocytes are subject to interactions between various Notch ligands and receptors, as well as proteins like those of the Fringe family, which regulate these interactions (19). A second checkpoint occurs at the transcriptional level, where Ikaros directly binds to Notch target sequences, presumably in competition with RBP-Jκ, to modulate the transcription of Notch target genes such as Hes-1. In DN4 cells, increased Ikaros levels compete with RBP-Jκ for binding and contribute to the deposition of silent epigenetic marks. As cells differentiate into DP cells, Ikaros levels and its binding to the Hes-1 promoter decrease, suggesting that silent chromatin marks no longer require Ikaros for repression. In contrast, in Ikaros-deficient DN4 cells, RBP-Jκ maintains greater access to Hes-1 regulatory elements, and transcription remains responsive to Notch signaling.

Our results thus establish Ikaros as a novel negative regulator of Notch signaling, which competes with RBP-Jκ for Notch target sequences. This mode of repression adds to the classical concept of RBP-Jκ-dependent repression, where RBP-Jκ binds to target sequences in the absence of Notch signaling and recruits corepressors such as MINT/SHARP (34, 40, 50). Ligand signals are thought to displace these repressive complexes and allow the assembly of the RBP-Jκ/NIC/Mastermind activator complex. While RBP-Jκ-dependent repression allows dynamic responses to ligand, Ikaros-mediated silencing would, on the other hand, prevent target gene transcription in the presence of Notch signaling. This additional silencing mechanism may be especially important in cells where accidental Notch signals can be oncogenic, like in developing T cells.

Ikaros deficiency leads to a marked decrease in H3K27 trimethylation at the Hes-1 promoter in DP thymocytes. How Ikaros modulates H3 methylation is unclear. It might reposition target loci to the vicinity of pericentromeric heterochromatin (9, 10, 36, 43), perhaps by molecular bridges with other Ikaros molecules bound to γ-satellite sequences (13), which could indirectly lead to methylation changes. Alternatively, Ikaros could directly regulate H3K27 methylation/demethylation factors. Further investigation is required to decipher the mechanisms downstream of Ikaros that leads to histone H3 methylation.

One relevant question is whether competition between Ikaros and RBP-Jκ is a common mode of regulation among Notch target genes. Our data indicate that this is true for at least two regions of the Hes-1 promoter. Furthermore, when reexpressed in $Ik^{L/L}$ leukemic T cells, Ikaros represses a large number of Notch target genes, such as Deltex-1, Ifi-204, and Meltrinβ (17 and our unpublished data), raising the possibility that Ikaros/RBP-Jκ competition regulates these genes. Recently, Screpanti and colleagues reported that Ikaros and RBP-Jκ competitively bind three TGGGAA motifs spaced 50 to 250 bp apart in the promoter of the pTα gene (5). However, using conditions that yield strong Ikaros or RBP-Jκ binding to Hes-1-derived probes, we detected only very weak Ikaros or RBP-Jκ binding to these sequences (E. Kleinmann, unpublished results). The physiological relevance of Ikaros/RBP-Jκ competition on the pTα promoter thus remains uncertain, especially since the proposed target motifs are not conserved across species (our unpublished observations). Thus, further investigation will be required to determine the relative importance of Ikaros/RBP-Jκ antagonism on Notch target gene tran-

scription. Interestingly, we have found that several Notch target genes, including Hes-1, are upregulated in $Ik^{L/L}$ bone marrow plasmacytoid dendritic cells (2), suggesting that Ikaros interferes with Notch signaling in other cell types. Lastly, Ikaros may compete with other factors such as early B-cell factor to silence target genes, as was recently proposed for the λ5 gene in immature B cells (48).

In summary, our results indicate that Ikaros competes with RBP-Jκ to repress the response of immature thymocytes to Notch signaling, resulting in histone methylation at target gene promoters. We propose that this mechanism is essential for turning off potentially harmful genes during the normal transition from DN to DP thymocytes.

ACKNOWLEDGMENTS

We thank J. C. Zuniga-Pflucker for the OP9-DL1 cells; A. Israel for the RBP-Jκ expression vector; L. Bianchetti for his help using PromAn and GeneDoc; P. Marchal for technical assistance; C. Ebel and J. Barths for help with flow cytometry; and S. Falcone and M. Gendron for animal husbandry.

This work was supported by institute funds from INSERM, CNRS, and the Hôpital Universitaire de Strasbourg. S.C. and P.K. received grants from the Association pour la Recherche sur le Cancer (ARC), the Fondation de France, the Ligue Nationale Française Contre le Cancer (LNCC; Equipe Labellisée), the Ligue Régionale (Haut-Rhin) Contre le Cancer, the Agence Nationale de la Recherche, and the Institut National du Cancer. E.K. received predoctoral fellowships from the LNCC and ARC. A.-S.G.L. received a predoctoral fellowship from the Ministère de la Recherche et de la Technologie. M.S. received a predoctoral fellowship from the Fondation pour la Recherche Médicale.

REFERENCES

1. **Allman, D., F. G. Karnell, J. A. Punt, S. Bakkour, L. Xu, P. Myung, G. A. Koretzky, J. C. Pui, J. C. Aster, and W. S. Pear.** 2001. Separation of Notch1 promoted lineage commitment and expansion/transformation in developing T cells. J. Exp. Med. **194:**99–106.
2. **Allman, D., M. Dalod, C. Asselin-Paturel, T. Delale, S. H. Robbins, G. Trinchieri, C. A. Biron, P. Kastner, and S. Chan.** 2006. Ikaros is required for plasmacytoid dendritic cell differentiation. Blood **108:**4025–4034.
3. **Andrews, N. C., and D. V. Faller.** 1991. A rapid micropreparation technique for extraction of DNA-binding proteins from limiting numbers of mammalian cells. Nucleic Acids Res. **19:**2499.
4. **Barolo, S., T. Stone, A. G. Bang, and J. W. Posakony.** 2002. Default repression and Notch signaling: Hairless acts as an adaptor to recruit the corepressors Groucho and dCtBP to Suppressor of Hairless. Genes Dev. **16:** 1964–1976.
5. **Bellavia, D., M. Mecarozzi, A. F. Campese, P. Grazioli, C. Talora, L. Frati, A. Gulino, and I. Screpanti.** 2007. Notch3 and the Notch3-upregulated RNA-binding protein HuD regulate Ikaros alternative splicing. EMBO J. **26:**1670–1680.
6. **Besseyrias, V., E. Fiorini, L. J. Strobl, U. Zimber-Strobl, A. Dumortier, U. Koch, M. L. Arcangeli, S. Ezine, H. R. Macdonald, and F. Radtke.** 2007. Hierarchy of Notch-Delta interactions promoting T cell lineage commitment and maturation. J. Exp. Med. **204:**331–343.
7. **Beverly, L. J., and A. J. Capobianco.** 2003. Perturbation of Ikaros isoform selection by MLV integration is a cooperative event in Notch(IC)-induced T cell leukemogenesis. Cancer Cell **3:**551–564.
8. **Bray, S. J.** 2006. Notch signalling: a simple pathway becomes complex. Nat. Rev. Mol. Cell Biol. **7:**678–689.
9. **Brown, K. E., J. Baxter, D. Graf, M. Merkenschlager, and A. G. Fisher.** 1999. Dynamic repositioning of genes in the nucleus of lymphocytes preparing for cell division. Mol. Cell **3:**207–217.
10. **Brown, K. E., S. S. Guest, S. T. Smale, K. Hahm, M. Merkenschlager, and A. G. Fisher.** 1997. Association of transcriptionally silent genes with Ikaros complexes at centromeric heterochromatin. Cell **91:**845–854.
11. **Choi, J. W., C. Pampeno, S. Vukmanovic, and D. Meruelo.** 2002. Characterization of the transcriptional expression of Notch-1 signaling pathway members, Deltex and HES-1, in developing mouse thymocytes. Dev. Comp. Immunol. **26:**575–588.
12. **Ciofani, M., G. C. Knowles, D. L. Wiest, H. von Boehmer, and J. C. Zuniga-Pflucker.** 2006. Stage-specific and differential notch dependency at the alphabeta and gammadelta T lineage bifurcation. Immunity **25:**105–116.
13. **Cobb, B. S., S. Morales-Alcelay, G. Kleiger, K. E. Brown, A. G. Fisher, and S. T. Smale.** 2000. Targeting of Ikaros to pericentromeric heterochromatin by direct DNA binding. Genes Dev. **14:**2146–2160.
14. **Correia-Neves, M., C. Waltzinger, J. M. Wurtz, C. Benoist, and D. Mathis.** 1999. Amino acids specifying MHC class preference in TCR V alpha 2 regions. J. Immunol. **163:**5471–5477.
15. **Cortes, M., E. Wong, J. Koipally, and K. Georgopoulos.** 1999. Control of lymphocyte development by the Ikaros gene family. Curr. Opin. Immunol. **11:**167–171.
16. **Deftos, M. L., E. Huang, E. W. Ojala, K. A. Forbush, and M. J. Bevan.** 2000. Notch1 signaling promotes the maturation of CD4 and CD8 SP thymocytes. Immunity **13:**73–84.
17. **Dumortier, A., R. Jeannet, P. Kirstetter, E. Kleinmann, M. Sellars, N. R. Dos Santos, C. Thibault, J. Barths, J. Ghysdael, J. A. Punt, P. Kastner, and S. Chan.** 2006. Notch activation is an early and critical event during T-cell leukemogenesis in Ikaros-deficient mice. Mol. Cell. Biol. **26:**209–220.
18. **Garbe, A. I., A. Krueger, F. Gounari, J. C. Zuniga-Pflucker, and H. von Boehmer.** 2006. Differential synergy of Notch and T cell receptor signaling determines alphabeta versus gammadelta lineage fate. J. Exp. Med. **203:** 1579–1590.
19. **Haines, N., and K. D. Irvine.** 2003. Glycosylation regulates Notch signalling. Nat. Rev. Mol. Cell Biol. **4:**786–797.
20. **Harker, N., T. Naito, M. Cortes, A. Hostert, S. Hirschberg, M. Tolaini, K. Roderick, K. Georgopoulos, and D. Kioussis.** 2002. The CD8alpha gene locus is regulated by the Ikaros family of proteins. Mol. Cell **10:**1403–1415.
21. **Harman, B. C., E. J. Jenkinson, and G. Anderson.** 2003. Microenvironmental regulation of Notch signalling in T cell development. Semin. Immunol. **15:**91–97.
22. **Hoebeke, I., M. De Smedt, I. Van de Walle, K. Reynvoet, G. De Smet, J. Plum, and G. Leclercq.** 2006. Overexpression of HES-1 is not sufficient to impose T-cell differentiation on human hematopoietic stem cells. Blood **107:**2879–2881.
23. **Huang, E. Y., A. M. Gallegos, S. M. Richards, S. M. Lehar, and M. J. Bevan.** 2003. Surface expression of Notch1 on thymocytes: correlation with the double-negative to double-positive transition. J. Immunol. **171:**2296–2304.
24. **Ishibashi, M., K. Moriyoshi, Y. Sasai, K. Shiota, S. Nakanishi, and R. Kageyama.** 1994. Persistent expression of helix-loop-helix factor HES-1 prevents mammalian neural differentiation in the central nervous system. EMBO J. **13:**1799–1805.
25. **Jarriault, S., C. Brou, F. Logeat, E. H. Schroeter, R. Kopan, and A. Israel.** 1995. Signalling downstream of activated mammalian Notch. Nature **377:** 355–358.
26. **Jenkinson, E. J., W. E. Jenkinson, S. W. Rossi, and G. Anderson.** 2006. The thymus and T-cell commitment: the right niche for Notch? Nat. Rev. Immunol. **6:**551–555.
27. **Kaneta, M., M. Osawa, K. Sudo, H. Nakauchi, A. G. Farr, and Y. Takahama.** 2000. A role for pref-1 and HES-1 in thymocyte development. J. Immunol. **164:**256–264.
28. **Kim, H. K., and G. Siu.** 1998. The notch pathway intermediate HES-1 silences CD4 gene expression. Mol. Cell. Biol. **18:**7166–7175.
29. **Kim, J., S. Sif, B. Jones, A. Jackson, J. Koipally, E. Heller, S. Winandy, A. Viel, A. Sawyer, T. Ikeda, R. Kingston, and K. Georgopoulos.** 1999. Ikaros DNA-binding proteins direct formation of chromatin remodeling complexes in lymphocytes. Immunity **10:**345–355.
30. **Kirstetter, P., M. Thomas, A. Dierich, P. Kastner, and S. Chan.** 2002. Ikaros is critical for B cell differentiation and function. Eur. J. Immunol. **32:**720–730.
31. **Koipally, J., A. Renold, J. Kim, and K. Georgopoulos.** 1999. Repression by Ikaros and Aiolos is mediated through histone deacetylase complexes. EMBO J. **18:**3090–3100.
32. **Krejcí, A., and S. Bray.** 2007. Notch activation stimulates transient and selective binding of Su(H)/CSL to target enhancers. Genes Dev. **21:**1322–1327.
33. **Krueger, A., and H. von Boehmer.** 2007. Identification of a T lineage-committed progenitor in adult blood. Immunity **26:**105–116.
34. **Kuroda, K., H. Han, S. Tani, K. Tanigaki, T. Tun, T. Furukawa, Y. Taniguchi, H. Kurooka, Y. Hamada, S. Toyokuni, and T. Honjo.** 2003. Regulation of marginal zone B cell development by MINT, a suppressor of Notch/RBP-J. signaling pathway. Immunity **18:**301–312.
35. **Lardenois, A., F. Chalmel, L. Bianchetti, J. A. Sahel, T. Leveillard, and O. Poch.** 2006. PromAn: an integrated knowledge-based web server dedicated to promoter analysis. Nucleic Acids Res. **34:**W578–W583.
36. **Liu, Z., P. Widlak, Y. Zou, F. Xiao, M. Oh, S. Li, M. Y. Chang, J. W. Shay, and W. T. Garrard.** 2006. A recombination silencer that specifies heterochromatin positioning and ikaros association in the immunoglobulin kappa locus. Immunity **24:**405–415.
37. **Murata, K., M. Hattori, N. Hirai, Y. Shinozuka, H. Hirata, R. Kageyama, T. Sakai, and N. Minato.** 2005. Hes1 directly controls cell proliferation through the transcriptional repression of p27Kip1. Mol. Cell. Biol. **25:**4262–4271.
38. **Nam, Y., P. Sliz, L. Song, J. C. Aster, and S. C. Blacklow.** 2006. Structural basis for cooperativity in recruitment of MAML coactivators to Notch transcription complexes. Cell **124:**973–983.

39. **Nam, Y., P. Sliz, W. S. Pear, J. C. Aster, and S. C. Blacklow.** 2007. Cooperative assembly of higher-order Notch complexes functions as a switch to induce transcription. Proc. Natl. Acad. Sci. USA **104:**2103–2108.
40. **Oswald, F., M. Winkler, Y. Cao, K. Astrahantseff, S. Bourteele, W. Knochel, and T. Borggrefe.** 2005. RBP-Jκ/SHARP recruits CtIP/CtBP corepressors to silence Notch target genes. Mol. Cell. Biol. **25:**10379–10390.
41. **Reizis, B., and P. Leder.** 2002. Direct induction of T lymphocyte-specific gene expression by the mammalian Notch signaling pathway. Genes Dev. **16:**295–300.
42. **Rothenberg, E. V.** 2007. Negotiation of the T lineage fate decision by transcription-factor interplay and microenvironmental signals. Immunity **26:**690–702.
43. **Sabbattini, P., M. Lundgren, A. Georgiou, C. Chow, G. Warnes, and N. Dillon.** 2001. Binding of Ikaros to the lambda5 promoter silences transcription through a mechanism that does not require heterochromatin formation. EMBO J. **20:**2812–2822.
44. **Sambandam, A., I. Maillard, V. P. Zediak, L. Xu, R. M. Gerstein, J. C. Aster, W. S. Pear, and A. Bhandoola.** 2005. Notch signaling controls the generation and differentiation of early T lineage progenitors. Nat. Immunol. **6:**663–670.
45. **Schmitt, T. M., and J. C. Zuniga-Pflucker.** 2002. Induction of T cell development from hematopoietic progenitor cells by delta-like-1 in vitro. Immunity **17:**749–756.
46. **Taghon, T. N., E. S. David, J. C. Zuniga-Pflucker, and E. V. Rothenberg.** 2005. Delayed, asynchronous, and reversible T-lineage specification induced by Notch/Delta signaling. Genes Dev. **19:**965–978.
47. **Tan, J. B., I. Visan, J. S. Yuan, and C. J. Guidos.** 2005. Requirement for Notch1 signals at sequential early stages of intrathymic T cell development. Nat. Immunol. **6:**671–679.
48. **Thompson, E. C., B. S. Cobb, P. Sabbattini, S. Meixlsperger, V. Parelho, D. Liberg, B. Taylor, N. Dillon, K. Georgopoulos, H. Jumaa, S. T. Smale, A. G. Fisher, and M. Merkenschlager.** 2007. Ikaros DNA-binding proteins as integral components of B cell developmental-stage-specific regulatory circuits. Immunity **26:**335–344.
49. **Tomita, K., M. Hattori, E. Nakamura, S. Nakanishi, N. Minato, and R. Kageyama.** 1999. The bHLH gene Hes1 is essential for expansion of early T cell precursors. Genes Dev. **13:**1203–1210.
50. **Tsuji, M., R. Shinkura, K. Kuroda, D. Yabe, and T. Honjo.** 2007. Msx2-interacting nuclear target protein (Mint) deficiency reveals negative regulation of early thymocyte differentiation by Notch/RBP-J. signaling. Proc. Natl. Acad. Sci. USA **104:**1610–1615.
51. **Weng, A. P., J. M. Millholland, Y. Yashiro-Ohtani, M. L. Arcangeli, A. Lau, C. Wai, C. Del Bianco, C. G. Rodriguez, H. Sai, J. Tobias, Y. Li, M. S. Wolfe, C. Shachaf, D. Felsher, S. C. Blacklow, W. S. Pear, and J. C. Aster.** 2006. c-Myc is an important direct target of Notch1 in T-cell acute lymphoblastic leukemia/lymphoma. Genes Dev. **20:**2096–2109.
52. **Winandy, S., L. Wu, J. H. Wang, and K. Georgopoulos.** 1999. Pre-T cell receptor (TCR) and TCR-controlled checkpoints in T cell differentiation are set by Ikaros. J. Exp. Med. **190:**1039–1048.
53. **Winandy, S., P. Wu, and K. Georgopoulos.** 1995. A dominant mutation in the Ikaros gene leads to rapid development of leukemia and lymphoma. Cell **83:**289–299.